Published in final edited form as:
Oncogene. 2009 November 12; 28(45): 4022–4033. doi:10.1038/onc.2009.253.

Hepatic tumor–stroma crosstalk guides epithelial to mesenchymal transition at the tumor edge

F van Zijl[1], **M Mair**[2], **A Csiszar**[3], **D Schneller**[1], **G Zulehner**[1], **H Huber**[1], **R Eferl**[2], **H Beug**[3], **H Dolznig**[4], and **W Mikulits**[1]

[1]Department of Medicine I, Division: Institute of Cancer Research, Medical University of Vienna, Vienna, Austria

[2]Ludwig Boltzmann Institute for Cancer Research, Vienna, Austria

[3]Research Institute of Molecular Pathology, Vienna, Austria

[4]Institute of Clinical Pathology, Medical University of Vienna, Vienna, Austria

Abstract

The tumor–stroma crosstalk is a dynamic process fundamental in tumor development. In hepatocellular carcinoma (HCC), the progression of malignant hepatocytes frequently depends on transforming growth factor (TGF)-β provided by stromal cells. TGF-β induces an epithelial to mesenchymal transition (EMT) of oncogenic Ras-transformed hepatocytes and an upregulation of platelet-derived growth factor (PDGF) signaling. To analyse the influence of the hepatic tumor–stroma crosstalk onto tumor growth and progression, we co-injected malignant hepatocytes and myofibroblasts (MFBs). For this, we either used *in vitro*-activated $p19^{ARF}$ MFBs or *in vivo*-activated MFBs derived from physiologically inflamed livers of $Mdr2/p19^{ARF}$ double-null mice. We show that co-transplantation of MFBs with Ras-transformed hepatocytes strongly enhances tumor growth. Genetic interference with the PDGF signaling decreases tumor cell growth and maintains plasma membrane-located E-cadherin and β-catenin at the tumor–host border, indicating a blockade of hepatocellular EMT. We further generated a collagen gel-based three dimensional HCC model *in vitro* to monitor the MFB-induced invasion of micro-organoid HCC spheroids. This invasion was diminished after inhibition of TGF-β or PDGF signaling. These data suggest that the TGF-β/PDGF axis is crucial during hepatic tumor–stroma crosstalk, regulating both tumor growth and cancer progression.

Keywords

TGF-β; PDGF; tumor–stroma interaction; epithelial to mesenchymal transition; spheroid

Introduction

Hepatocellular carcinoma (HCC) represents the sixth most common cancer worldwide with a still increasing incidence (Parkin *et al.,* 2005). Independent on the various risk factors, HCC most frequently involves preceding inflammation, liver fibrosis and cirrhosis, the latter

Correspondence: Professor W Mikulits, Department of Medicine I, Division: Institute of Cancer Research, Medical University of Vienna, Borschke-Gasse 8a, Vienna A-1090, Austria. wolfgang.mikulits@meduniwien.ac.at.

Conflict of interest
The authors declare no conflict of interest.

Supplementary Information accompanies the paper on the Oncogene website (http://www.nature.com/onc)

Europe PMC Funders Author Manuscripts

is considered as the pre-malignant hepatic condition (Friedman, 2004; Sherman, 2005). In fact, more than 80% of HCC develops in pathological settings of both chronic hepatitis and cirrhosis during persisting regeneration of hepatocytes, which promotes genetic and epigenetic alterations (Kensler *et al.,* 2003; Lee and Thorgeirsson, 2005).

The interaction of malignant hepatocytes with non-parenchymal, stromal liver cells is crucial in liver carcinoma progression. Myofibroblasts (MFBs) are central in the hepatic tumor–stroma crosstalk by their modulation of extracellular matrix, fibrogenesis and chemoattraction of leukocytes (Iredale, 2007). Hepatic MFBs mostly originate through activation of hepatic stellate cells (HSCs, also called Ito cells) and portal fibroblasts (Knittel *et al.*, 1999; Geerts, 2001; Magness *et al.*, 2004). Furthermore, bone-marrow-derived mesenchymal stem cells contribute to the MFB population during liver injury (Forbes *et al.*, 2004; Kisseleva *et al.*, 2006; Russo *et al.*, 2006), and also non-malignant hepatocytes can convert into MFB-like cells (Ikegami *et al.*, 2007; Zeisberg *et al.*, 2007; Dooley *et al.*, 2008). The expression of α-smooth muscle actin (α-SMA) and glial fibrillary acidic protein (GFAP) are characteristic for hepatic MFBs derived from HSCs, and indicate chronic liver injury (Ramadori *et al.*, 1990; Gabbiani, 2003). MFBs are involved in extracellular matrix remodeling through increased synthesis of interstitial collagen type I and III, as well as expression of matrix metalloproteases and tissue inhibitors of matrix metalloproteases (Knittel *et al.*, 1992; Roderfeld *et al.*, 2006). Furthermore, secretion of chemokines, such as monocyte chemoattractant protein (MCP)-1 (also known as Chemokine (C-C motif) ligand 2 (CCL-2)), by activated HSCs accounts for chemoattraction of monocytes and contribute to the inflammatory infiltration of activated Kupffer cells (Sprenger *et al.*, 1999; Marra, 2002).

The tumor microenvironment-controlled reprogramming of cytokine and chemokine networks during hepatocarcinogenesis is still poorly understood (Witz, 2008). Transforming growth factor (TGF)-β—the strongest pro-fibrotic cytokine, which promotes the transition of HSCs to MFBs—enhances HCC progression through a paracrine mechanism, which is abrogated by inhibition of TGF-β/Smad signaling in hepatocytes (Gressner *et al.*, 2002; Mikula *et al.*, 2006). Platelet-derived growth factor (PDGF), the strongest proliferation-inducing cytokine of HSCs, represents a further potent stimulus in the hepatic tumor microenvironment (Pinzani *et al.*, 1996). MFBs regulate TGF-β and PDGF production through autocrine mechanisms, and are therefore a potential source that might contribute to HCC progression (Ostman and Heldin, 2001; Campbell *et al.*, 2005, 2007). It remained unclear whether, and to what extent, PDGF produced by activated HSCs and MFBs contribute to HCC development. Interestingly, about 70% of HCC patients display upregulated levels of PDGF receptor-α (PDGF-Rα) in malignant hepatocytes, suggesting a significant role of PDGF signaling in human HCC (Stock *et al.*, 2007).

Multiple mechanisms are involved in the progression of HCC, including (i) activation of mitogen-activated protein kinase (MAPK) signaling (Tsuboi *et al.*, 2004; Amann *et al.*, 2009), (ii) sustained stimulation of TGF-β signaling (Rossmanith and Schulte-Hermann, 2001; Breuhahn *et al.*, 2006) and (iii) nuclear accumulation of β-catenin (Lee *et al.*, 2006a). In parallel, HCC progression frequently associates with an epithelial to mesenchymal transition (EMT) of hepatocytes caused by the collaboration of STAT5b with the hepatitis B protein, HBX, or by the cooperation of laminin 5 and TGF-β (Giannelli *et al.*, 2005; Lee *et al.*, 2006b). In addition, EMT has been reported to occur in cirrhotic liver-derived hepatocytes that exhibited enhanced cell survival dependent on MAPK signaling (Nitta *et al.*, 2008). EMT is well known in embryonic development, but has been recently recognized as a central event in cancer progression, leading to an invasive, mesenchymal-like phenotype important for tumor cell spreading and metastatic dissemination (Thiery and Sleeman, 2006; Moustakas and Heldin, 2007).

A typical hallmark of EMT in both mouse and human HCC is the disruption of E-cadherin/β-catenin complexes followed by nuclear translocation of stabilized β-catenin (Gotzmann *et al.*, 2002; Giannelli *et al.*, 2005). A common mechanism to induce EMT and invasiveness involves the cooperation of TGF-β with Ras/MAPK signaling (Gotzmann *et al.*, 2002; Grunert *et al.*, 2003), stabilized by the establishment of an autocrine TGF-β loop. Interestingly, EMT induced by the synergy of oncogenic Ras plus TGF-β in murine MIM hepatocytes involves the upregulation of PDGF-Rs to establish autocrine PDGF signaling (Fischer *et al.*, 2007; Lahsnig *et al.*, 2009). Induction of hepatocellular EMT through TGF-β secreted by MFBs underscores the essential role of the hepatic microenvironment in modulating the invasive behavior of HCC cells (Mikula *et al.*, 2006). Therefore, investigating the molecular and cellular mechanisms underlying the tumor–stroma crosstalk is of fundamental importance for understanding HCC progression.

Here, we studied the TGF-β- and PDGF-dependent tumor–stroma interaction in a disease-relevant, murine HCC model *in vivo* as well as in a three dimension (3D) micro-organoid HCC model *in vitro*. The data suggest a crucial role for the TGF-β/PDGF signaling axis in controlling both tumor growth and progression involving EMT at the tumor–host border.

Results

MFBs enhance tumor growth associated with Ras/MAPK signaling

To analyse the impact of the microenvironment on tumor growth and progression, we performed co-transplantation of neoplastic hepatocytes and liver myofibroblastoid cells *in vivo*. Subcutaneous rather than orthotopic co-injection was conducted to avoid influence on hepatocytes exerted by other hepatic cell types. More specifically, non-tumorigenic myofibroblastoid cells derived from activated HSCs by long-term treatment with TGF-β (M-HT; Proell *et al.*, 2005) were co-transplanted with MIM-hepatocytes either expressing oncogenic Ha-Ras (MIM-R) or MIM-R overexpressing dominant-negative (dn) PDGF-Rα (MIM-R-dnP; Fischer *et al.*, 2007). MIM-R hepatocytes alone formed fivefold larger tumors than MIM-R-dnP cells alone (Figure 1a), in agreement with our recently published findings (Fischer *et al.*, 2007). Co-transplantation of either MIM-R or MIM-R-dnP hepatocytes together with myofibroblastoid M-HT cells strongly accelerated tumor growth, resulting in threefold and fourfold larger tumor volumes as compared with those generated by MIM-R and MIM-R-dnP cells alone, respectively (Figure 1a). As expected, tumor weights closely corresponded to tumor volumes (Figure 1b). As a control, M-HT cells injected alone failed to induce tumor formation (data not shown).

Next, we analysed the involvement of MAPK and phosphoinositide 3-kinase signaling in tumor growth stimulated by MFBs. For this, MIM hepatocytes expressing the Ras mutants, S35-V12-Ras (MIM-S35) and C40-V12-Ras (MIM-C40), were employed, showing selective hyperactivation of extracellular signal-regulated kinase/MAPK and phosphoinositide 3-kinase/protein kinase B signaling, respectively (Fischer *et al.*, 2005). Whereas MIM-C40 hepatocytes did not show any tumor formation (data not shown), MIM-S35 cells generated larger tumors (Figure 1c; Fischer *et al.*, 2005) than did MIM-R cells (Figure 1a). Similarly, MIM-S35 hepatocytes co-expressing the dn PDGF-Rα (MIM-S35-dnP) showed reduced tumor size than did MIM-S35 control cells (Figure 1c), again in accordance with recent studies (Fischer *et al.*, 2007). Co-transplantation of both MIM-S35 and MIM-S35-dnP hepatocytes with M-HT cells resulted in strong increase of tumor volumes, closely reflected by final tumor weights (Figure 1d).

Taken together, these data indicate that tumor generation from oncogene-transformed hepatocytes strongly depends on PDGF/PDGF-R signaling (Figures 1a and b; dark gray versus white bars). In contrast, the significant increase in tumor growth caused by co-

transplanted MFBs might be due to PDGF-R-independent mechanisms. MAPK-activated MIM-S35 hepatocytes are prone to develop tumors earlier as compared with MIM-R hepatocytes, whereas MIM-C40 cells were not tumorigenic at all, indicating that MAPK but not phosphoinositide 3-kinase signaling is essential for Ras-activated tumor development in MIM hepatocytes.

We next addressed the fate of M-HT myofibroblastoid cells during tumor formation after their co-transplantation with MIM-R hepatocytes. M-HT cells immortalized from $p19^{ARF}$ null mice express markers specific for hepatic MFBs, such as α-SMA, GFAP, desmin and fibulin-2 (Sasaki *et al.*, 1996; Morini *et al.*, 2005). Furthermore, M-HT MFBs proliferate in culture but are not tumorigenic *in vivo* (Proell *et al.*, 2005; Mikula *et al.*, 2006). Immunohistochemical (IHC) analysis of serial tumor sections of co-transplanted tumors revealed that MFBs establish strands of proliferating cell nuclear antigen-positive cells within the tumors, surrounded by green fluorescent protein-positive hepatic tumor cells (Supplementary Figure 1a). Indeed, MFBs present in tumors expressed desmin, fibulin-2 and GFAP (Supplementary Figure 1b). Moreover, immunofluorescence of tumors arising from red fluorescent protein-expressing M-HT fibroblasts co-transplanted with green fluorescent protein-expressing MIM-R showed that few exogenous MFBs are still detectable 21 days after injection (Supplementary Figure 1c). In conclusion, the increase of tumor formation caused by co-transplantation of hepatocytes and MFBs is most probably dependent on their reciprocal proliferative stimulation as MFBs injected alone do not show any tumor formation.

The tumor-promoting effect of inflammation-induced MFBs

To verify the impact of stromal fibroblasts on tumor growth in a more physiological setting, we established MFBs derived from inflammation-induced hepatic fibrosis *in vivo*. For this, we crossbred Mdr2 null mice, which spontaneously develop hepatic inflammation and severe fibrosis (Fickert *et al.*, 2004), with $p19^{ARF}$ null mice allowing us to immortalize the respective MFBs. As expected, 4-week-old $Mdr2/p19^{ARF}$ double-null mice showed a phenotype comparable with Mdr2 null control mice, including periductal fibrosis and vast accumulation of MFBs around enlarged bile ducts. In contrast, bile ducts from control $p19^{ARF}$ null mice resembled wild-type tissues (Supplementary Figure 2a). Isolation of hepatic non-parenchymal cells 4-weeks postnatal resulted in a homogenous population of $Mdr2/p19^{ARF}$ double-null myofibroblastoid cells, referred to as Mdr2-p19, which showed expression of the hepatic MFB markers α-SMA, GFAP, desmin and fibulin-2 (Supplementary Figure 2b). In contrast to MFBs isolated from Mdr2 null mice, which started to degenerate after 5 days in culture, Mdr2-p19 MFBs showed proliferation and expansion into mass cultures (Supplementary Figure 2c).

MIM-R or MIM-R-dnP hepatocytes were then co-transplanted with Mdr2-p19 MFBs. To avoid a conceivable loss of inflammation-induced activation of the Mdr2-p19 MFBs on prolonged tissue culture, they were already used after 14 days of culturing. Rather than performing co-transplantations at a hepatocyte to MFB ratio of 1:10 (as done for MIM-R and M-HT cells), hepatocytes were co-injected with Mdr2-p19 cells at a ratio of 1:4 because of lower cell numbers available at the desired conditions. Co-transplantation of malignant cells with Mdr2-p19 MFBs resulted in a moderate increase of tumor volumes as compared with MIM-R or MIM-R-dnP alone (Figure 2a). Again, tumor weights corresponded to tumor volumes (Figure 2b). As expected, increased proliferation of malignant hepatocytes from either MIM-R- or MIM-R-dnP-derived tumors could be detected in the presence of M-HT or Mdr2-p19 MFBs by quantification of Ki-67-positive cell nuclei (Figures 2c and d). Similar to M-HT MFBs, Mdr2-p19 cells were non-tumorigenic when transplanted alone (data not shown). Taken together, co-transplantation with MFBs isolated from the inflamed liver

verified the enhancement of tumor growth by the hepatic stroma, confirming their tumor promoting role in HCC.

PDGF signaling is necessary for maintenance of EMT at the tumor–host border of experimental HCC

Intact PDGF/PDGF-R signaling was crucial for tumor growth in HCC, as intervention with PDGF-R resulted in lower tumor volumes (Figures 1 and 2). We next assessed whether paracrine PDGF signaling was also important for tumor progression. As tumor progression is based on soluble, auto- or paracrine cytokines, we first measured secretion of TGF-β and PDGF, proposed as key regulatory cytokines within tumor–stroma crosstalk (Bhowmick *et al.*, 2004; Pollard, 2004; de Visser and Coussens, 2006). As expected, *in vitro* TGF-β treatment of MIM-R and MIM-S35 hepatocytes with or without dn-PDGF-R expression stimulated autocrine TGF-β-production in all cell types (Figure 3a). PDGF-AA secretion was massively induced on TGF-β treatment in all cell types except in MIM-S35-dnP cells (Figure 3b). Interestingly, interfering with PDGF-R resulted in a decrease of PDGF-AA secretion, verifying an autocrine loop. Importantly, *in vivo*-activated fibroblasts (Mdr2-p19) showed a threefold higher secretion of TGF-β1 (Figure 3c) and a higher secretion of PDGF-AA (Figure 3d) than *in vitro*-activated fibroblasts (M-HT), although the latter feature was rapidly lost under cell culture conditions. Secretion of PDGF-AB or PDGF-BB could hardly be detected in these cells (data not shown).

These data verify that TGF-β-dependent activation of autocrine PDGF secretion and PDGF-R signaling is essential for experimental HCC development and progression (Gotzmann *et al.*, 2006; Fischer *et al.*, 2007). It is therefore very likely that MFB-produced, paracrine TGF-β and PDGF cause the observed tumor-promoting effects of co-transplanted MFBs. Accordingly, we examined the expression of PDGF-Rα in tumor sections by IHC staining. Elevated levels of PDGF-Rα were predominantly observed in regions close to the tumor edge, whereas the tumor center was less strongly stained or even devoid of PDGF-Rα expression (Supplementary Figure 3a). Overexpression of Smad7, a protein inhibiting TGF-β signaling, abolished PDGF-Rα expression in MIM-R cells throughout the tumor, indicating an essential role of TGF-β signaling in PDGF-R expression at the tumor–host border (Supplementary Figure 3a). The over-expression of Smad7 in respective cells has been confirmed by quantitative reverse transcriptase PCR (Supplementary Figure 3b).

To assess the role of PDGF/PDGF-R signaling during tumor progression, as indicated by EMT at the tumor–host border, we next performed IHC staining with various EMT markers in serial tumor sections. At the edge of tumors arising from MIM-R alone or MIM-R co-transplanted with M-HT, green fluorescent protein-positive tumor cells underwent EMT by losing membrane-localized E-cadherin and β-catenin, while showing elevated levels of non-destructible, nuclear β-catenin (Figure 4; T,t). In contrast, the tumor centers showed a heterogeneous pattern of epithelial and mesenchymal characteristics (Supplementary Figure 4). As an internal control, distinct plasma membrane-localized E-cadherin and β-catenin were observed in the epidermal keratinocytes (Figure 4, S,s). These data indicate that EMT of neoplastic hepatocytes predominantly occurs at the tumor edge, involving disruption of E-cadherin-dependent cell adhesion and nuclear translocation of β-catenin, which was accompanied by co-expression of the β-catenin target gene, $p16^{INK4A}$ (Supplementary Figure 5a). In addition, malignant MIM-R hepatocytes showed induction of the mesenchymal marker α-SMA and loss of the epithelial constituent p120-catenin ($p120^{ctn}$) at the tumor–host border, which both underline EMT (Supplementary Figure 5b).

In contrast, tumors generated by MIM-R-dnP alone or by MIM-R-dnP co-transplanted with M-HT failed to show EMT signatures at the tumor–host border (Figure 5 and Supplementary Figure 5b). In particular, both E-cadherin and total β-catenin were detected at plasma

membranes of most, if not all, neoplastic hepatocytes in the tumor (Figure 5, Supplementary Figure 6). This indicates that EMT, induced at the edge of respective MIM-R-derived tumors, was efficiently inhibited by suppression of PDGF-R-signaling. IHC staining of tumors arising from co-transplantation with Mdr2-p19 MFBs verified those findings (Figure 6). Whereas MIM-R cells undergo EMT at the tumor–host border, MIM-R-dn-P cells maintained an epithelial phenotype because of interference with PDGF signaling. Unexpectedly, nuclear β-catenin (ABC) was detected in all combinations and independent of ablating PDGF signaling (Figures 4-6), suggesting that certain aspects of EMT occurred in the presence of dnP. This could either be due to incomplete blockade of PDGF signaling by expression of dnP or due to PDGF-independent mechanisms activating two distinct isoforms of β-catenin (Gottardi and Gumbiner, 2004; Herzig *et al.*, 2007). In conclusion, the vast impact of the host can induce EMT of malignant MIM-R cells at the tumor edge, independent of co-transplantation of MFBs. Interfering with PDGF signaling abrogates this invasive phenotype at the tumor–host border, indicating that intact PDGF signaling is crucial for maintenance of TGF-β-induced EMT for further invasion and metastasis.

MFBs induce local invasion

The above results showed that tumor–stroma interaction with murine skin did induce EMT in malignant hepatocytes dependent on an intact PDGF signaling, whereas co-transplanted activated MFBs strongly enhanced tumor growth, but did not show a clear effect on EMT formation. To study the impact of MFBs in a distinct, spatially extended tumor–stroma interface without interference of the host, we developed a 3D micro-organoid *in vitro* tumor model. In this assay, tumor spheroids were prepared from 100 MIM-R cells and co-cultivated with MFBs in the surrounding gel. MIM-R spheroids alone showed proliferation in 3D gels and an epithelial phenotype. The spheroids were even able to fuse, while maintaining their epithelial characteristics (Figure 7a, left panel). Co-cultivation of spheroids with adjacent Mdr2-p19 fibroblasts induced strong invasion of tumor cells into the gel. These cells lost their epithelial phenotype, as indicated by loss of plasma membrane-bound E-cadherin (Figure 7a, middle panel), β-catenin and ZO-1 (zona occludens) (Supplementary Figure 7). Interestingly, these changes in marker localization occurred while cells of spheroids scattered and gained mesenchymal features, that is, the ability of detaching from each other and invading into the gel as single cells (Figure 7a; arrows). The effect of this tumor–stroma interaction was completely abolished by employing the TGF-β receptor inhibitor, LY02109761 (Lahsnig *et al.*, 2009), which restored a compact spheroid morphology and plasma membrane expression of E-cadherin (Figure 7a), ZO-1 and β-catenin (Supplementary Figure 7). Inhibition of PDGF signaling by Imatinib (STI 571) was only partially able to block the MFB-induced dispersion and invasion of tumor spheroids. PDGF-R inhibition resulted in cells invading the collagen gels, but never detaching from each other and maintaining their epithelial characteristics such as plasma membrane expression of E-cadherin (Figure 7a), ZO-1 and β-catenin (Supplementary Figure 7). To verify the role of TGF-β and PDGF on cell invasion, we incubated MIM-R spheroids with recombinant TGF-β, PDGF or with supernatant of Mdr2-p19 MFBs. As expected, PDGF alone could not induce EMT (data not shown), whereas TGF-β and conditioned medium provoked cell invasion by displaying cord-like structures and EMT, which was associated with destruction of membrane-bound β-catenin (data not shown), E-cadherin and stress fibre formation (Figure 7b). Taken together, these data confirm that the tumor–stroma interaction is crucial for tumor development, wherein TGF-β induces and PDGF maintains EMT at the tumor–host border.

Discussion

In this study, we analysed the crosstalk between malignant hepatocytes and MFBs in a co-transplantation model *in vivo*, with the particular focus on TGF-β and PDGF signaling. We show by genetic intervention that PDGF signaling is necessary for both tumor growth and maintenance of EMT at the tumor–host border. The latter finding was corroborated in a 3D micro-organoid HCC model *in vitro*, in which MFB-induced tumor cell invasion was diminished after pharmacological intervention with TGF-β or PDGF signaling. These results indicate a crucial role of the TGF-β/PDGF axis in both hepatocellular tumor growth and progression.

Tumor growth factor-β represents one of the most potent cytokines produced by the tumor–stroma, which induces or enhances the expression of PDGF-Rs and the secretion of PDGF-AA in hepatocytes (Figure 3, Gotzmann *et al.*, 2006) and other tumor models (Jechlinger *et al.*, 2006). The cooperation between TGF-β and MAPK signaling is crucial for the induction of EMT and the survival of hepatocytes during tumor progression. Here, we show that PDGF-Rα is essential for tumor growth of HCC as well as for maintenance of EMT at the tumor edge, whereas initiation of EMT requires TGF-β signaling.

We also were interested to identify further cytokines important for the hepatic tumor progression. Vascular endothelial growth factor (VEGF) induces neoangiogenesis and, thus, promotes tumor growth and progression (Bissell and Radisky, 2001; Pardali and Moustakas, 2007), and has been shown to be stimulated by TGF-β at the mRNA level (Benckert *et al.,* 2003). We observed an increased VEGF secretion of myofibroblastoid Mdr2-p19 compared with M-HT (Supplementary Figure 8a) and a TGF-β-dependent secretion of VEGF-A in malignant Ras-expressing hepatocytes (Supplementary Figure 8b). However, no differences in blood vessel density were detected, neither by IHC staining with the panendothelial marker, MECA-32, nor by staining with VEGF-R2.

An important role of PDGF during tumor–stroma interaction is the regulation and modulation of immune cell function. TGF-β inhibits proliferation and differentiation of B- and T lymphocytes, and thus establishes an immune-suppressive microenvironment (Pardali and Moustakas, 2007), but tumors frequently escape this immune surveillance and even proliferate through factors produced by activated immune cells (de Visser and Coussens, 2006). At sites of wound healing, macrophages are recruited and can potentiate tumor cell proliferation and progression by secretion of matrix metalloproteases and cytokines such as TGF-β, fibroblast growth factor-2 and PDGF (Bissell and Radisky, 2001). We observed a time- and context-dependent impact of inflammation and fibrosis on liver tumor progression, as Mdr2-p19 MFBs, isolated at the first peak of inflammation (Fickert *et al.*, 2004), show elevated CCL-2/MCP-1 secretion (Supplementary Figure 8c). Secreted CCL-2/MCP-1 might recruit immune cells, such as macrophages, which contribute to early phases of the immune response. In contrast, M-HT cells develop from HSCs that have undergone long-term treatment with TGF-β, and show elevated CCL-5/ Rantes secretion (Supplementary Figure 8d) typical for later stages of inflammation. Secreted CCL-5/Rantes might attract B- and T cells and enhance metastatic abilities of the tumor (De Wever *et al.*, 2008). However, we examined tumor–stroma interactions in an immune-suppressed microenvironment of SCID (severe combined immunodeficient) mice.

We propose that the reciprocal tumor–stroma interactions enhance liver tumor growth and progression. During early stages of hepatocarcinogenesis, TGF-β released from nonparenchymal compartments, such as immune cells, causes the transdifferentiation of HSCs and portal fibroblasts to MFBs, which then secrete TGF-β and PDGF (Supplementary Figure 9). TGF-β induces EMT of neoplastic hepatocytes in cooperation with MAPK

signaling, and at the same time stimulates autocrine production of PDGF, which maintains EMT. Resulting malignant hepatocytes produce both TGF-β and PDGF, which in turn stimulate the microenvironment to further generate and attract hepatic MFBs. Cytokines and chemokines produced by these MFBs, such as CCL-2/MCP-1 and CCL-5/Rantes, attract immune cells (Supplementary Figure 9). In summary, liver fibrosis and cirrhosis generate activated MFBs that are crucial for HCC development. These MFBs provoke malignant hepatocytes to undergo EMT at the tumor edge and thus render them capable to invade and metastasize. Targeting the TGF-β/PDGF axis in this context could be a promising way to interfere with both tumor cells and MFBs to efficiently combat hepatocarcinogenesis.

Material and methods

Cell culture

Immortalized $p19^{ARF}$ null hepatocytes (MIM) expressing oncogenic Ha-Ras, termed MIM-R, the mutants, S35-V12-Ras and C40-V12-Ras, referred to as MIM-S35 and MIM-C40, respectively (Fischer *et al.*, 2005), as well as those co-expressing the dn-PDGF-Rα (MIM-R-dnP and MIM-S35-dnP) were cultured as described (Fischer *et al.*, 2007). Myofibroblastoid cell types from $p19^{ARF}$ null mice (M-HT, Proell *et al.*, 2005), M-HT expressing red fluorescent protein, as well as those isolated from Mdr2 null and Mdr2/$p19^{ARF}$ double-null mice (referred to as Mdr2 and Mdr2-p19, respectively) were grown on tissue culture plastic in Dulbecco's modified Eagle's media supplemented with 10% fetal calf serum and antibiotics. M-HT myofibroblastoid cells derived from HSCs (M1-4HSC) after long-term treatment with TGF-β1 were continuously supplied with 1 ng/ml TGF-β1 (R&D Systems, Minneapolis, USA). All cells were kept at 37 °C and 5% CO_2, and routinely screened for the absence of mycoplasma.

Co-transplantation and tumor formation in vivo

In total, 1×10^5 cells of each malignant cell type (MIMR, MIM-S35, MIM-C40, MIM-R-dnP or MIM-S35-dnP) were mixed in 100 μl medium either with myofibroblastoid M-HT or with Mdr2-p19 cells in a ratio of 1:10 or 1:4, respectively, and subcutaneously injected into three individual SCID/BALB/c recipient mice as outlined recently (Mikula *et al.*, 2006). As control, each cell line (1×10^5) was subcutaneously inoculated alone and tumor volumes were calculated as described (Gotzmann *et al.*, 2002). Tumor incidences were equal to 100%. Tumors were surgically removed 3 weeks after injection and processed for further analysis. Experiments were performed in triplicate to quadruplets, and carried out according to the Austrian guidelines for animal care and protection.

Immunohistochemistry

Experimental tumors were fixed in 4% formaldehyde/phosphate-buffered saline. Paraffin-embedded tissues were cut into 4 μm-thick sections and stained with hematoxylin and eosin or trichrome (Sigma, St Louis, USA). The following primary antibodies were used at a dilution of 1:100: anti-proliferating cell nuclear antigen (Dako, Carpintera, USA), anti-β-catenin and anti-E-cadherin (Transduction Laboratories, Lexington, UK), anti-active-β-catenin (clone 8E7, Upstate, Lake Palcid, USA), anti-α-SMA (Dako, Glostrup, Denmark), anti-green fluorescent protein (Santa Cruz Biotechnology, Santa Cruz, CA, USA), anti-PDGF-Rα (NeoMarkers, Fremont, CA, USA), anti-desmin (Clone D33, Dako), anti-GFAP (Dako), anti-fibulin-2 (kindly provided by Dr T Sasaki), anti-$p16^{INK4A}$ (Santa Cruz Biotechnology), anti-$p120^{ctn}$ (BD Transduction laboratories, Franklin Lakes, NJ, USA) and anti-Ki-67 (Novocastra, Newcastle, UK). Subsequently, corresponding biotinylated secondary antibodies were applied, and visualization was carried out with the vectastain ABC kit (Vector Laboratories, Burlingame, USA).

3D micro-organoid murine HCC model

Spheroid formation and incubation was performed as described (Dolznig *et al.*, submitted). Briefly, for spheroid formation, single cell suspension (100 cells per 100 μl) in RPMI containing 20% methyl cellulose (Sigma) was incubated for 2 days at 37 °C and 5% CO_2. After harvesting, 96 spheroids were mixed alone or with 2×10^5 MFBs (Mdr2-p19) in collagen I (Sigma) and plated into plastic jigs to harden at 37 °C. Subsequently, gels were transferred into a 24-well plate and incubated with medium at cell culture conditions as outlined. 2.5 ng/ml TGF-β1 (R&D Systems) or supernatant of Mdr2-p19 MFBs were employed in spheroid cultures as indicated.

Confocal immunofluorescence microscopy of spheroids

Collagen gels were fixed in 4% formaldehyde/phosphate-buffered saline for 10 min at room temperature. After blocking for 30 min (1% phosphate-buffered saline/0.5% Tween 20/0.2% fish gelatine with 0.2 μg/ ml IgG1) at room temperature, 200 μl of the following primary antibodies (dilution 1:100–1:300) were applied and incubated overnight at 4 °C: anti-β-catenin, anti-E-cadherin (Transduction Laboratories), Texas Red-X phalloidin (Invitrogen, Carlsbad, CA, USA) and anti-ZO-1 (Invitrogen). The corresponding secondary antibody was diluted in phosphate-buffered saline Tween 20/0.2% gelatine and 200 μl of the mixture per gel were incubated for 2 h. Imaging was performed by confocal microscopy (Zeiss, Jena, Germany).

Enzyme-linked immunosorbent assay

Cells were grown in serum-free Dulbecco's modified Eagle's media or RPMI containing 10 mM HEPES (4-(2-hydroxyethyl)-1-piperazineethanesulfonic acid) and antibiotics for 24 h. Subsequently, conditioned super-natants were harvested and cell numbers were determined by CASY cell counter (Schärfe Systems, Reutlingen, Germany). Enzyme-linked immunosorbent assays were performed in triplicate using the mouse total TGF-β1 or PDGF immunoassays (R&D Systems) as well as the VEGF-A, MCP-1 or RANTES immunoas-says according to the instructions of the manufacturer (Bender MedSystems, Vienna, Austria). All values were normalized to respective growth media. Values of secreted proteins are expressed per 1×10^6 cells per ml supernatant.

Statistical analysis

Data are expressed as means±standard error of the median (s.e.m.). The statistical significance of differences was evaluated using unpaired, non-parametric Student's *t*-test.

Supplementary Material

Refer to Web version on PubMed Central for supplementary material.

Acknowledgments

Mdr2 null mice were kindly provided by Dr Ilan Stein. We thank Dr Takako Sasaki for the fibulin-2 antibody. This work was supported by the Austrian Science Fund, FWF, grant numbers P19598-B13 (to WM) and SFB F28 (to RE, HB and WM), the 'Hochschuljubiläumsstiftung der Stadt Wien' (to WM), the Herzfelder Family Foundation (to WM), and the European Union, FP7 Health Research, project number HEALTH-F4-2008-202047 (to WM).

References

Amann T, Bataille F, Spruss T, Muhlbauer M, Gabele E, Scholmerich J, et al. Activated hepatic stellate cells promote tumorigenicity of hepatocellular carcinoma. Cancer Sci. 2009; 100:646–653. [PubMed: 19175606]

Benckert C, Jonas S, Cramer T, Von Marschall Z, Schafer G, Peters M, et al. Transforming growth factor beta 1 stimulates vascular endothelial growth factor gene transcription in human cholangiocellular carcinoma cells. Cancer Res. 2003; 63:1083–1092. [PubMed: 12615726]

Bhowmick NA, Neilson EG, Moses HL. Stromal fibroblasts in cancer initiation and progression. Nature. 2004; 432:332–337. [PubMed: 15549095]

Bissell MJ, Radisky D. Putting tumours in context. Nat Rev Cancer. 2001; 1:46–54. [PubMed: 11900251]

Breuhahn K, Longerich T, Schirmacher P. Dysregulation of growth factor signaling in human hepatocellular carcinoma. Oncogene. 2006; 25:3787–3800. [PubMed: 16799620]

Campbell JS, Hughes SD, Gilbertson DG, Palmer TE, Holdren MS, Haran AC, et al. Platelet-derived growth factor **C** induces liver fibrosis, steatosis, and hepatocellular carcinoma. Proc Natl Acad Sci USA. 2005; 102:3389–3394. [PubMed: 15728360]

Campbell JS, Johnson MM, Bauer RL, Hudkins KL, Gilbertson DG, Riehle KJ, et al. Targeting stromal cells for the treatment of platelet-derived growth factor **C**-induced hepatocellular carcinogenesis. Differentiation. 2007; 75:843–852. [PubMed: 17999742]

de Visser KE, Coussens LM. The inflammatory tumor microenvironment and its impact on cancer development. Contrib Microbiol. 2006; 13:118–137. [PubMed: 16627962]

De Wever O, Demetter P, Mareel M, Bracke M. Stromal myofibroblasts are drivers of invasive cancer growth. Int J Cancer. 2008; 123:2229–2238. [PubMed: 18777559]

Dooley S, Hamzavi J, Ciuclan L, Godoy P, Ilkavets I, Ehnert S, et al. Hepatocyte-specific Smad7 expression attenuates TGF-beta-mediated fibrogenesis and protects against liver damage. Gastroenterology. 2008; 135:642–659. [PubMed: 18602923]

Fickert P, Fuchsbichler A, Wagner M, Zollner G, Kaser A, Tilg H, et al. Regurgitation of bile acids from leaky bile ducts causes sclerosing cholangitis in Mdr2 (Abcb4) knockout mice. Gastroenterology. 2004; 127:261–274. [PubMed: 15236191]

Fischer AN, Fuchs E, Mikula M, Huber H, Beug H, Mikulits W. PDGF essentially links TGF-beta signaling to nuclear beta-catenin accumulation in hepatocellular carcinoma progression. Oncogene. 2007; 26:3395–3405. [PubMed: 17130832]

Fischer AN, Herrera B, Mikula M, Proell V, Fuchs E, Gotzmann J, et al. Integration of Ras subeffector signaling in TGF-beta mediated late stage hepatocarcinogenesis. Carcinogenesis. 2005; 26:931–942. [PubMed: 15705598]

Forbes SJ, Russo FP, Rey V, Burra P, Rugge M, Wright NA, et al. A significant proportion of myofibroblasts are of bone marrow origin in human liver fibrosis. Gastroenterology. 2004; 126:955–963. [PubMed: 15057733]

Friedman SL. Mechanisms of disease: mechanisms of hepatic fibrosis and therapeutic implications. Nat Clin Pract Gastroenterol Hepatol. 2004; 1:98–105. [PubMed: 16265071]

Gabbiani G. The myofibroblast in wound healing and fibrocontractive diseases. J Pathol. 2003; 200:500–503. [PubMed: 12845617]

Geerts A. History, heterogeneity, developmental biology, and functions of quiescent hepatic stellate cells. Semin Liver Dis. 2001; 21:311–335. [PubMed: 11586463]

Giannelli G, Bergamini C, Fransvea E, Sgarra C, Antonaci S. Laminin-5 with transforming growth factor-beta1 induces epithelial to mesenchymal transition in hepatocellular carcinoma. Gastroenterology. 2005; 129:1375–1383. [PubMed: 16285938]

Gottardi CJ, Gumbiner BM. Distinct molecular forms of beta-catenin are targeted to adhesive or transcriptional complexes. J Cell Biol. 2004; 167:339–349. [PubMed: 15492040]

Gotzmann J, Fischer AN, Zojer M, Mikula M, Proell V, Huber H, et al. A crucial function of PDGF in TGF-beta-mediated cancer progression of hepatocytes. Oncogene. 2006; 25:3170–3185. [PubMed: 16607286]

Gotzmann J, Huber H, Thallinger C, Wolschek M, Jansen B, Schulte-Hermann R, et al. Hepatocytes convert to a fibroblastoid phenotype through the cooperation of TGF-beta1 and Ha-Ras: steps towards invasiveness. J Cell Sci. 2002; 115:1189–1202. [PubMed: 11884518]

Gressner AM, Weiskirchen R, Breitkopf K, Dooley S. Roles of TGF-beta 1 in hepatic fibrosis. Front Biosci. 2002; 7:d793–d807. [PubMed: 11897555]

Grunert S, Jechlinger M, Beug H. Diverse cellular and molecular mechanisms contribute to epithelial plasticity and metastasis. Nat Rev Mol Cell Biol. 2003; 4:657–665. [PubMed: 12923528]

Herzig M, Savarese F, Novatchkova M, Semb H, Christofori G. Tumor progression induced by the loss of E-cadherin independent of beta-catenin/Tcf-mediated Wnt signaling. Oncogene. 2007; 26:2290–2298. [PubMed: 17043652]

Ikegami T, Zhang Y, Matsuzaki Y. Liver fibrosis: possible involvement of EMT. Cells Tissues Organs. 2007; 185:213–221. [PubMed: 17587827]

Iredale JP. Models of liver fibrosis: exploring the dynamic nature of inflammation and repair in a solid organ. J Clin Invest. 2007; 117:539–548. [PubMed: 17332881]

Jechlinger M, Sommer A, Moriggl R, Seither P, Kraut N, Capodiecci P, et al. Autocrine PDGFR signaling promotes mammary cancer metastasis. J Clin Invest. 2006; 116:1561–1570. [PubMed: 16741576]

Kensler TW, Qian GS, Chen JG, Groopman JD. Translational strategies for cancer prevention in liver. Nat Rev Cancer. 2003; 3:321–329. [PubMed: 12724730]

Kisseleva T, Uchinami H, Feirt N, Quintana-Bustamante O, Segovia JC, Schwabe RF, et al. Bone marrow-derived fibrocytes participate in pathogenesis of liver fibrosis. J Hepatol. 2006; 45:429–438. [PubMed: 16846660]

Knittel T, Kobold D, Saile B, Grundmann A, Neubauer K, Piscaglia F, et al. Rat liver myofibroblasts and hepatic stellate cells: different cell populations of the fibroblast lineage with fibrogenic potential. Gastroenterology. 1999; 117:1205–1221. [PubMed: 10535885]

Knittel T, Schuppan D, Meyer zum Buschenfelde KH, Ramadori G. Differential expression of collagen types I, III, and IV by fat-storing (Ito) *cells in vitro*. Gastroenterology. 1992; 102:1724–1735. [PubMed: 1373696]

Lahsnig C, Mikula M, Petz M, Zulehner G, Schneller D, van Zijl F, et al. ILEI requires oncogenic Ras for the epithelial to mesenchymal transition of hepatocytes and liver carcinoma progression. Oncogene. 2009; 28:638–650. [PubMed: 19015638]

Lee HC, Kim M, Wands JR. Wnt/Frizzled signaling in hepatocellular carcinoma. Front Biosci. 2006a; 11:1901–1915. [PubMed: 16368566]

Lee JS, Thorgeirsson SS. Genetic profiling of human hepatocellular carcinoma. Semin Liver Dis. 2005; 25:125–132. [PubMed: 15918141]

Lee TK, Man K, Poon RT, Lo CM, Yuen AP, Ng IO, et al. Signal transducers and activators of transcription 5b activation enhances hepatocellular carcinoma aggressiveness through induction of epithelial-mesenchymal transition. Cancer Res. 2006b; 66:9948–9956. [PubMed: 17047057]

Magness ST, Bataller R, Yang L, Brenner DA. A dual reporter gene transgenic mouse demonstrates heterogeneity in hepatic fibrogenic cell populations. Hepatology. 2004; 40:1151–1159. [PubMed: 15389867]

Marra F. Chemokines in liver inflammation and fibrosis. Front Biosci. 2002; 7:d1899–d1914. [PubMed: 12161342]

Mikula M, Proell V, Fischer AN, Mikulits W. Activated hepatic stellate cells induce tumor progression of neoplastic hepatocytes in a TGF-beta dependent fashion. J Cell Physiol. 2006; 209:560–567. [PubMed: 16883581]

Morini S, Carotti S, Carpino G, Franchitto A, Corradini SG, Merli M, et al. GFAP expression in the liver as an early marker of stellate cells activation. Ital J Anat Embryol. 2005; 110:193–207. [PubMed: 16536051]

Moustakas A, Heldin CH. Signaling networks guiding epithelial-mesenchymal transitions during embryogenesis and cancer progression. Cancer Sci. 2007; 98:1512–1520. [PubMed: 17645776]

Nitta T, Kim JS, Mohuczy D, Behrns KE. Murine cirrhosis induces hepatocyte epithelial mesenchymal transition and alterations in survival signaling pathways. Hepatology. 2008; 48:909–919. [PubMed: 18712785]

Ostman A, Heldin CH. Involvement of platelet-derived growth factor in disease: development of specific antagonists. Adv Cancer Res. 2001; 80:1–38. [PubMed: 11034538]

Pardali K, Moustakas A. Actions of TGF-beta as tumor suppressor and pro-metastatic factor in human cancer. Biochim Biophys Acta. 2007; 1775:21–62. [PubMed: 16904831]

Parkin DM, Bray F, Ferlay J, Pisani P. Global cancer statistics, 2002. CA Cancer J Clin. 2005; 55:74–108. [PubMed: 15761078]

Pinzani M, Milani S, Herbst H, DeFranco R, Grappone C, Gentilini A, et al. Expression of platelet-derived growth factor and its receptors in normal human liver and during active hepatic fibrogenesis. Am J Pathol. 1996; 148:785–800. [PubMed: 8774134]

Pollard JW. Tumour-educated macrophages promote tumour progression and metastasis. Nat Rev Cancer. 2004; 4:71–78. [PubMed: 14708027]

Proell V, Mikula M, Fuchs E, Mikulits W. The plasticity of p19 ARF null hepatic stellate cells and the dynamics of activation. Biochim Biophys Acta. 2005; 1744:76–87. [PubMed: 15878400]

Ramadori G, Veit T, Schwogler S, Dienes HP, Knittel T, Rieder H, et al. Expression of the gene of the alpha-smooth muscle-actin isoform in rat liver and in rat fat-storing (ITO) cells. Virchows Arch B Cell Pathol Incl Mol Pathol. 1990; 59:349–357. [PubMed: 1705733]

Roderfeld M, Weiskirchen R, Wagner S, Berres ML, Henkel C, Grotzinger J, et al. Inhibition of hepatic fibrogenesis by matrix metalloproteinase-9 mutants in mice. FASEB J. 2006; 20:444–454. [PubMed: 16507762]

Rossmanith W, Schulte-Hermann R. Biology of transforming growth factor beta in hepatocarcinogenesis. Microsc Res Tech. 2001; 52:430–436. [PubMed: 11170302]

Russo FP, Alison MR, Bigger BW, Amofah E, Florou A, Amin F, et al. The bone marrow functionally contributes to liver fibrosis. Gastroenterology. 2006; 130:1807–1821. [PubMed: 16697743]

Sasaki T, Wiedemann H, Matzner M, Chu ML, Timpl R. Expression of fibulin-2 by fibroblasts and deposition with fibronectin into a fibrillar matrix. J Cell Sci. 1996; 109(Part 12):2895–2904. [PubMed: 9013337]

Sherman M. Hepatocellular carcinoma: epidemiology, risk factors, and screening. Semin Liver Dis. 2005; 25:143–154. [PubMed: 15918143]

Sprenger H, Kaufmann A, Garn H, Lahme B, Gemsa D, Gressner AM. Differential expression of monocyte chemotactic protein-1 (MCP-1) in transforming rat hepatic stellate cells. J Hepatol. 1999; 30:88–94. [PubMed: 9927154]

Stock P, Monga D, Tan X, Micsenyi A, Loizos N, Monga SP. Platelet-derived growth factor receptor-alpha: a novel therapeutic target in human hepatocellular cancer. Mol Cancer Ther. 2007; 6:1932–1941. [PubMed: 17604334]

Thiery JP, Sleeman JP. Complex networks orchestrate epithelial-mesenchymal transitions. Nat Rev Mol Cell Biol. 2006; 7:131–142. [PubMed: 16493418]

Tsuboi Y, Ichida T, Sugitani S, Genda T, Inayoshi J, Takamura M, et al. Overexpression of extracellular signal-regulated protein kinase and its correlation with proliferation in human hepatocellular carcinoma. Liver Int. 2004; 24:432–436. [PubMed: 15482339]

Witz IP. Yin-yang activities and vicious cycles in the tumor microenvironment. Cancer Res. 2008; 68:9–13. [PubMed: 18172289]

Zeisberg M, Yang C, Martino M, Duncan MB, Rieder F, Tanjore H, et al. Fibroblasts derive from hepatocytes in liver fibrosis via epithelial to mesenchymal transition. J Biol Chem. 2007; 282:23337–23347. [PubMed: 17562716]

Europe PMC Funders Author Manuscripts

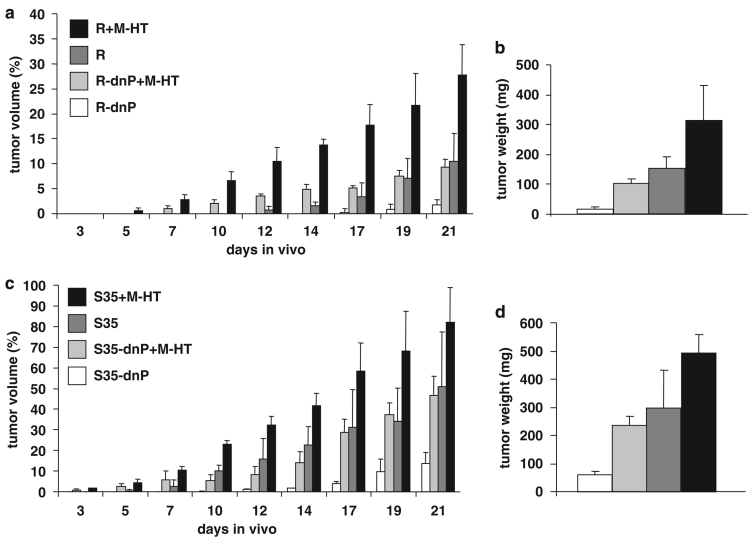

Figure 1.

Myofibroblasts enhance tumor formation of neoplastic hepatocytes *in vivo*. 1×10^5 malignant hepatocytes were injected either alone or in combination with M-HT fibroblasts at a ratio of 1 (hepatocytes) to 10 (M-HT) into SCID (severe combined immunodeficient) mice. Tumor formation was followed by measuring tumor volumes, expressed as percent of the highest level obtained (100% is equal to 1 cm^3). After 21 days, animals were killed, and tumor tissues were collected and weighed. (**a**) Tumor formation of MIM-R (R) and MIM-R-dnP (R-dnP) hepatocytes in the absence and presence of M-HT myofibroblastoid cells. (**b**) Tumor weights corresponding to cell transplantations described in (**a**). (**c**) Tumor formation of MIM-S35 (S35) and MIM-S35-dnP (S35-dnP) hepatocytes with and without M-HT myofibroblastoid cells. (**d**) Tumor weights corresponding to cell transplantations described in (**c**). The statistical differences between kinetics of tumor formation were highly significant ($P<0.005$), except the differences between R and R-dnP+M-HT, as well as between S35 and S35-dnP+M-HT. Error bars denote s.e.m. Similar results were obtained in three further independent experiments. Each sample was injected into three mice per experiment. dnP, dominant-negative platelet-derived growth factor receptor-α; M-HT, hepatic stellate cells long-term treated with TGF-β; MIM-R, $p19^{ARF}$ null hepatocytes overexpressing Ha-Ras; MIM-S35, $p19^{ARF}$ null hepatocytes expressing the mutant S35-V12-Ras.

Europe PMC Funders Author Manuscripts

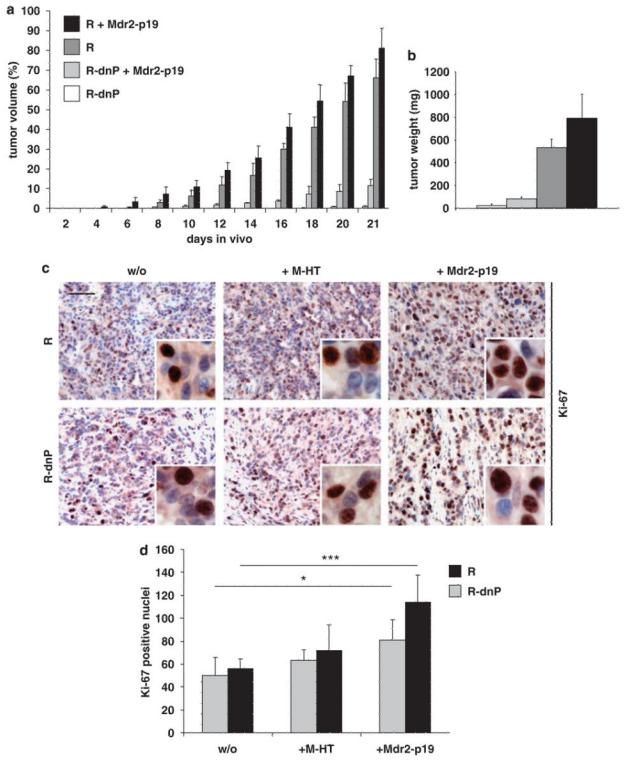

Figure 2.

Inflammation-induced myofibroblastoid cells enhance tumor proliferation of neoplastic hepatocytes *in vivo*. A total of 1×10^5 MIM-R hepatocytes were injected alone or in combination with Mdr2-p19 myofibroblasts at a ratio of 1:4 into SCID (severe combined immunodeficient) mice. Tumor formation was measured and depicted as in Figure 1. (**a**) Tumor formation of MIM-R (R) and MIM-R-dnP (R-dnP) hepatocytes in the absence and presence of Mdr2-p19 myofibroblastoid cells. (**b**) Tumor weights corresponding to cell transplantations described in (**a**). The difference between R-dnP and R-dnP+Mdr2-p19 was statistically highly significant ($P<0.005$) Each sample was injected into three mice per experiment. One representative experiment out of five is shown. (**c**) Ki-67 immunohistochemical staining of tumors generated from MIM-R (R) or MIM-R-dnP (R-dnP) hepatocytes alone (w/o) or co-transplanted with either M-HT (+M-HT) or with Mdr2-p19 fibroblasts (+Mdr2-p19). Insets show cells at higher magnification. (**d**) Quantitative evaluation of Ki-67-positive nuclei of four regions in three independent tumors each. $*P<0.05$; $***P<0.005$; Error bars denote s.e.m. Scale bar, 50 μm. Mdr2-p19, myofibroblasts isolated from $p19^{ARF}$/Mdr2 double-null livers.

Europe PMC Funders Author Manuscripts

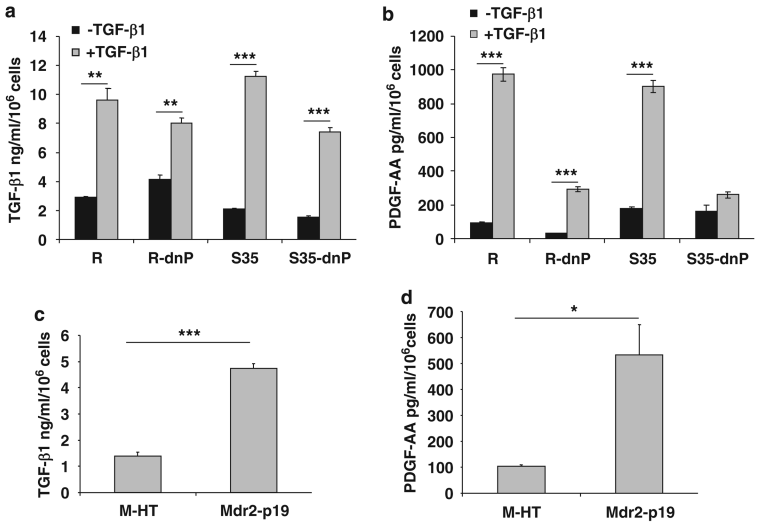

Figure 3.

Transforming growth factor-β (TGF-β) and platelet-derived growth factor (PDGF) secretion in the hepatic tumor microenvironment. Amounts of secreted TGF-β1 and PDGF-AA were determined in triplicate and plotted as nanogram and picogram per millilitre supernatant per 10^6 cells, respectively. (**a**) TGF-β stimulation of malignant hepatocytes induces their TGF-β secretion, suggesting induction of an autocrine TGF-β loop. (**b**) As a downstream event, TGF-β strongly induces PDGF-AA secretion, except in MIM-S35-dn-P cells, in which induction is less than twofold and not significant. PDGF-AA secretion is lowered by interfering with PDGF receptor (PDGF-R), verifying an autocrine PDGF loop. (**c**) *in vivo*-activated myofibroblasts (Mdr2-p19) show higher levels of secreted TGF-β1 and (**d**) PDGF-AA than *in vitro*-activated fibroblasts (M-HT). Comparable results were obtained in another independent experiment **P*<0.05; ***P*<0.01; ****P*<0.005.

Europe PMC Funders Author Manuscripts

Europe PMC Funders Author Manuscripts

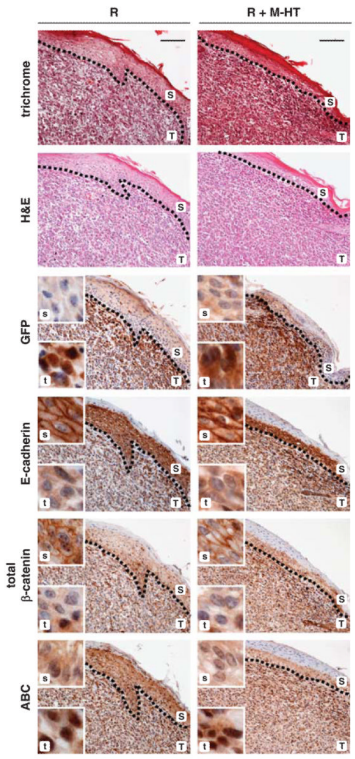

Figure 4.

Induction of epithelial to mesenchymal transition (EMT) at the tumor–host border. Tumor tissues were collected 21 days after co-transplantation of MIM-R hepatocytes alone (R) or in combination with M-HT myofibroblasts (R+M-HT). Serial sections of tumor tissues were used to display both tumor architecture (T,t) and skin (epidermis) morphology (S,s) by standard histology (trichrome and hematoxylin/eosin (H&E) staining), and immunohistochemical staining was performed to visualize EMT markers. Tumor sections were stained with anti-green fluorescent protein antibody to distinguish between murine skin (S,s) and exogenous, subcutaneous MIM-R hepatocytes (T,t). Dashed lines depict tumor-host borders. In the tumor cells, loss of the epithelial markers E-cadherin and total β-catenin from the plasma membrane and the accumulation of nuclear β-catenin (ABC) indicate an EMT at the tumor–host border. Insets show tumor (t) and skin (s) sections at higher magnification. Murine skin serves as internal control for staining. Scale bar, 100 μm. Dashed lines indicate tumor–host borders.

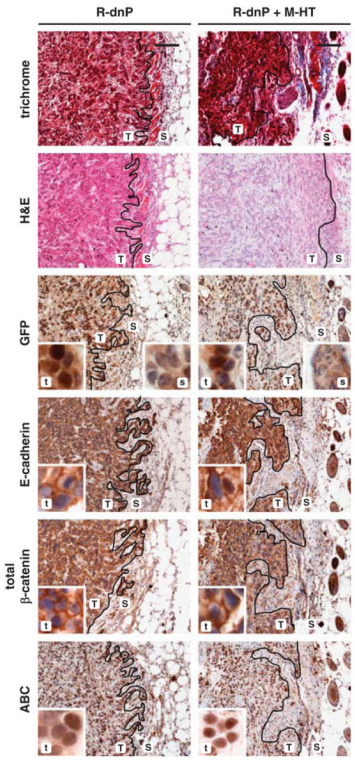

Figure 5.

Hepatocellular epithelial to mesenchymal transition (EMT) at the tumor–host interface is impaired by ablation of platelet-derived growth factor (PDGF) signaling. Tumor tissues collected 21 days after co-transplantation of MIM-R-dnP hepatocytes alone (R-dnP) or in combination with M-HT myofibroblasts (R-dnP+M-HT) were processed for standard histology and immunohistochemical staining on serial sections. Labeling of tumor (T,t) and epidermal (S,s) regions were done as in Figure 4. Staining of persistent plasma membrane-bound E-cadherin and β-catenin indicate a blockade of EMT at the tumor edge. Insets (t,s) show staining sections at higher magnification. Black lines indicate tumor–host borders. Scale bar, 100 μm.

Europe PMC Funders Author Manuscripts

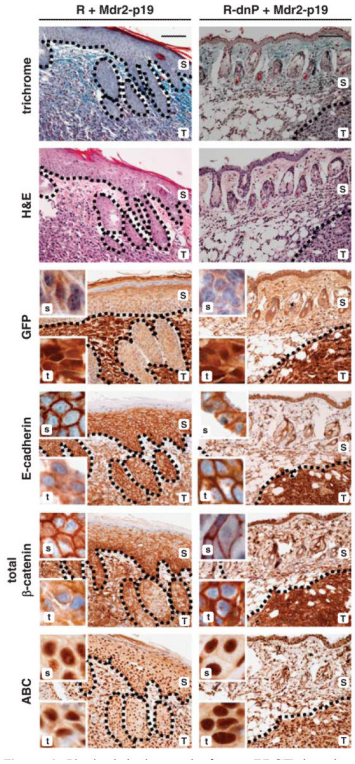

Figure 6.

Platelet-derived growth factor (PDGF)-dependent hepatocellular epithelial to mesenchymal transition (EMT) at the tumor–host interface after co-transplantation of inflammation-induced myofibroblastoid cells. MIM-R (R) or MIM-R-dnP (R-dnP) hepatocytes were co-transplanted with Mdr2-p19 myofibroblasts and tumor tissues were processed for standard histology and immunohistochemical staining on serial sections. MIM-R+Mdr2-p19-derived tumors (left panel; T,t) show loss of plasma membrane-localized E-cadherin and total β-catenin, as well as nuclear translocation of active β-catenin (ABC) at the tumor–host border, indicating EMT. In tumors arising from MIM-R-dnP+Mdr2-p19 (right panel; T,t), the blockade of PDGF-Rα signaling prevented EMT at the tumor edge, depicted by persistence of plasma membrane-bound E-cadherin and total β-catenin staining. Murine skin provides positive staining controls for epithelial characteristics (S,s). Insets (t,s) show staining of tumor sections at higher magnification. Dashed lines indicate tumor–host borders. Scale bar, 100 μm.

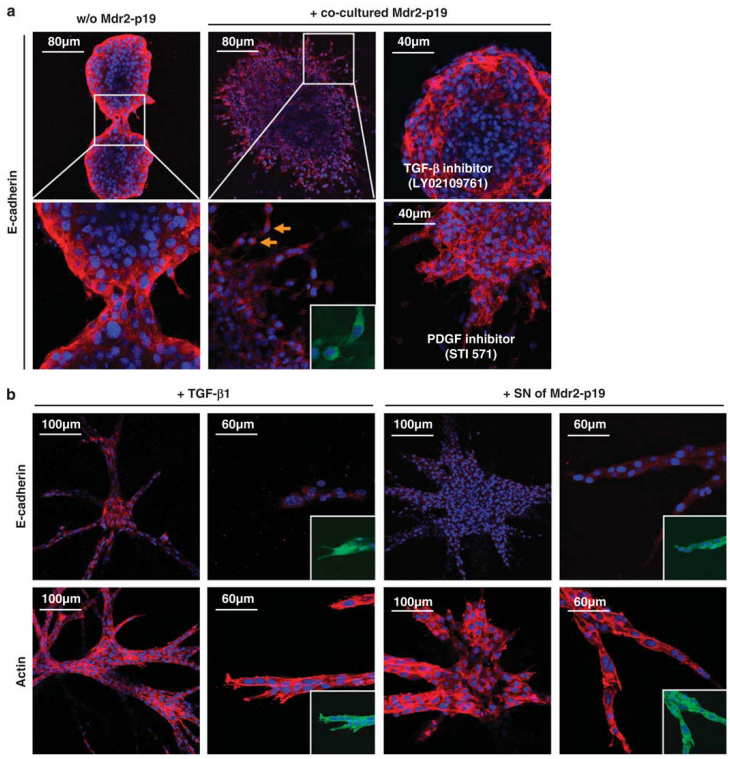

Figure 7.

Myofibroblasts provoke invasion of malignant hepatocytes. Three-dimensional micro-organoid tumor tissues were employed to study the molecular crosstalk between malignant hepatocytes and their associated myofibroblasts. (a) Immunofluorescent staining of E-cadherin (red) was performed to monitor epithelial organization, cell nuclei were counterstained with Hoechst dye (blue) and green fluorescent protein (GFP) of MIM-R was visualized (green, inset). MIM-R spheroids alone (w/o Mdr2-p19) show intact epithelial structures depicted by plasma membrane-bound E-cadherin, which is still persistent while two spheroids fuse into one (left panels). Co-cultivation of MIM-R spheroids with Mdr2-p19 myofibroblasts in the surrounding gel induced dispersion of spheroids and invasion of GFP-positive MIM-R hepatocytes (middle panels). Cytoplasmic E-cadherin indicates loosening of cell–cell contacts and detachment of GFP-positive single cells (arrows). Incubation with the TGF-β inhibitor, LY02109761 (20 μM), abrogated this epithelial to mesenchymal transition (EMT)-like process, yielding compact spheroids expressing plasma membrane-bound E-cadherin (upper right panel). Treatment with the platelet-derived growth factor receptor (PDGF-R) inhibitor STI 571 (Imatinib; 5 μM) resulted in persistent epithelial structures and partial inhibition of invasion (lower right panel). (b) Incubation of MIM-Ras spheroids with either TGF-β1 (2.5 ng/ml, left panels) or supernatant (SN) of Mdr2-p19 myofibroblasts induced both extensive invasion into the gel, depicted by loss of membrane-bound E-cadherin (red, upper panel), and rearrangement of the cytoskeleton depicted by actin (red, lower panel). Insets show GFP fluorescence. For each constitution, one representative spheroid out of a minimum of 100 spheroids is shown.